

Theoretical bounds on a non-raster scan method for tracking string-like samples

Peter I. Chang and Sean B. Andersson

Department of Mechanical Engineering
Boston University, Boston, MA 02215
{itchang,sanderss}@bu.edu

Abstract—In this paper, we study the performance of a non-raster-scan algorithm for imaging string-like samples in an atomic force microscope. The algorithm yields high-speed imaging through a feedback control law that steers the tip along the sample, thereby reducing the imaging time by eliminating unnecessary measurements. Under simplifying assumptions, we derive expressions for bounds on the control parameters to ensure accurate tracking of the sample.

I. INTRODUCTION

The invention of atomic force microscopy (AFM) in 1986 [1] has led to remarkable discoveries in the field of nanotechnology, molecular biology and many other areas. AFM is well suited to probe into the biological world at the molecular level due to its high spatial resolution and ability to operate in liquid. This capability has been brought to bear to improve our understanding of a wide variety of biomolecular structures, such as proteins, DNA, lipid films, molecular motors and others [2]–[4]. Despite these successes, the applicability of AFM to study the dynamics in systems with nanometer-scale features is extremely limited. In most commercial systems the time to collect a single image is measured in seconds to minutes. Because of the wealth of dynamic phenomena with time scales much faster than this, there is great interest in improving the temporal resolution of the instrument.

Researchers have brought many control applications to this problem [5]. Recent results in high speed AFM are approaching video rates [6]–[8]. These techniques rely on improving the control of the piezoelectric actuators used to achieve scanning to increase the scan rate of the system while maintaining imaging quality. Our approach takes a complementary approach and relies on developing high-level feedback control laws to steer the tip of the system so as to reduce the total number of data points acquired without reducing the amount of information gathered. The imaging time is

reduced by limiting the area that needs to be imaged. In earlier work we proposed a non-raster scan method for samples that are string-like [9]. More recently, the authors of this paper have modified this approach to a continuous scanning pattern based on the non-raster scan method [10]. Under this scheme the data measured by the AFM is used in real-time to steer the tip and track the string-like sample. This paper presents a theoretical analysis of the limits for guaranteeing imaging of a string-like sample.

In this paper, we will first discuss the background of our non-raster approach to scanning and describe the scenario in which tracking can be lost. In Section III we derive the full problem statement for the determining bounds on the control parameters to ensure the sample is not lost. In Section III-B we consider a worst case scenario and finally derive a concise algebraic expression in Section IV through a conservative approximation.

II. NON-RASTER SCAN METHOD

A. General Description

The basic idea, illustrated in Figure 1, on the non-raster scan method is to feedback the information gathered from the AFM tip and steer the tip in close proximity to the underlying sample. Below we briefly describe the approach; the details of this method can be found in [10].

Initially, the AFM tip is raster-scanned across the substrate until the sample is encountered. The (unknown) sample is modeled as a planar curve, denoted x_{tr} . To track the path defined by the sample, we need to estimate x_{tr} with the past information we have, and evolve this curve forward in the plane. We called this predicted path, the curve of *desired* sample trajectory, denoted x_d . Its spatial evolution is modeled using the equations for the evolution of a two dimensional Frenet-

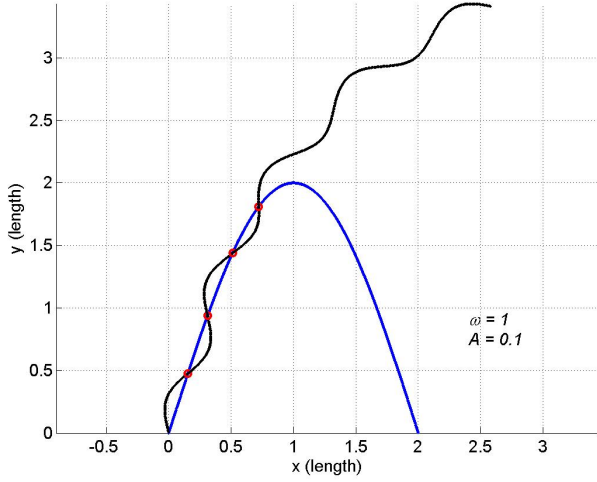


Fig. 3. Example of loss of tracking by sharp turn of sample. Here the AFM tip trajectory fails to intersect the sample and diverges from the true curve..

but with different arclength parameters, denoted s_d and s_{tr} respectively. Note that we set κ_d and κ_{tr} to be constant over a small arclength, so that x_d and x_{tr} are both segments of circular curves.

To determine the bounds we make the following assumptions.

- 1) The two trajectories start at the same place, designated as the origin:

$$x_{tip}|_{s_d=0} = x_{tr}|_{s_{tr}=0} = [0, 0]'$$

- 2) The two trajectories have the same tangent direction q_1 and normal direction q_2 at the origin:

$$\begin{aligned} q_{1tip}|_{s_d=0} &= q_{1tr}|_{s_{tr}=0} = [1, 0]' \\ q_{2tip}|_{s_d=0} &= q_{2tr}|_{s_{tr}=0} = [0, 1]' \end{aligned}$$

- 3) We set the arclength parameters s_d and s_{tr} to zero at the origin.

Based on the two curves, there are six unknowns involved in finding the bound to guarantee tracking. These are A , ω , κ_d , κ_{tr} , s_d and s_{tr} .

A. General Equation Setup

There are two conditions for x_{tip} and x_{tr} to meet. The first is that where the two trajectories must intersect. We call this the “point match” condition. The second is that at the location where the two intersect, the tangent directions must match. We call this the “tangent match” condition. The two conditions guarantee

that the two trajectories intersect at only a single point. These conditions can be mathematically expressed as:

$$x_{tip}(s_d) = x_{tr}(s_{tr}), \quad (3a)$$

$$\arctan\left(\frac{d}{ds_d}x_{tip}\right) = \arctan\left(\frac{d}{ds_{tr}}x_{tr}\right). \quad (3b)$$

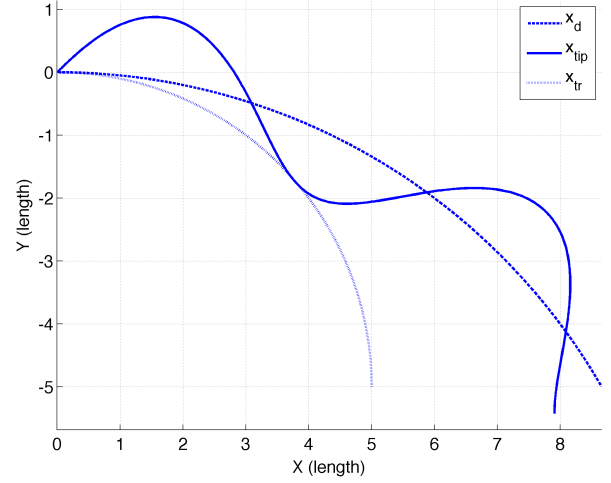


Fig. 4. Full problem setup for the limiting case of tracking a string-like sample. The true sample trajectory, shown dashed, is just about to leave the AFM tip trajectory, shown solid. At this point, the two trajectories must satisfy the “point match” and “tangent match” conditions in (3).

We demonstrate the scenario in Fig. (4). Here A is set to one unit length and ω is one rad/length. The tip trajectory x_{tip} in the figure is just touching the underlying trajectory x_{tr} . Note that the matching conditions of (3) must be met within the first cycle for the sinusoidal term in (2) and thus $\omega s_d \in [0, 2\pi]$.

Substituting (2) into (3a), and (1) into (3b), we can rewrite the matching conditions as:

$$x_{tr}(s_{tr}) = x_d(s_d) + A \sin(\omega s_d) q_{2d}(s_d) \quad (4a)$$

$$\begin{aligned} \arctan(q_{1tr}) &= \arctan[q_{1d} \\ &\quad - A\kappa_d \sin(\omega s_d) q_{1d} \\ &\quad + A\omega \cos(\omega s_d) q_{2d}]. \end{aligned} \quad (4b)$$

We also have an equation linking the two arclength parameters s_d and s_{tr} at this limiting condition. This can be derived using the geometric relationship shown in Fig. 5. From the figure, θ_d and θ_{tr} can be related by:

$$\tan \theta_d = \frac{\sin \theta_{tr}}{\cos \theta_{tr} + 1/\kappa_d - 1/\kappa_{tr}}$$

When we substitute $s = \theta/\kappa$ for the two arclength parameters, we arrive at:

$$s_d \kappa_d = \arctan \left(\frac{\sin(s_{tr} \kappa_{tr})}{\cos(s_{tr} \kappa_{tr}) + 1/\kappa_d - 1/\kappa_{tr}} \right). \quad (5)$$

The equations (4) and (5) yield a total of four independent equations: two from the vector equation in (4a), and the additional two from (4b) and (5). To solve them we must choose values for two of the unknowns and solve for the others. While the equations can be solved numerically, due to their complexity, they yield very little insight on finding values for the control parameters A and ω . We therefore next consider a limiting case.

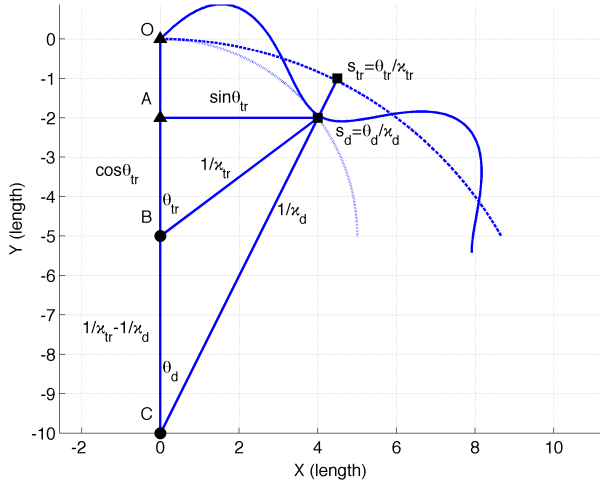


Fig. 5. Geometric relationship between the two arclength parameters s_d and s_{tr} using θ_d and θ_{tr} . In $\triangle s_d A C$, $\tan \theta_d$ can be found dividing the length $s_d A = \sin \theta_{tr}$ and $A C = \cos \theta_{tr} + 1/\kappa_d - 1/\kappa_{tr}$.

B. Straight Line Case

Consider the two cases illustrated in Fig. 6. The straight line case has a lower tolerance for deviations of the true trajectory; that is a smaller difference between the true curvature and the predicted curvature (equal to zero in the straight line case) will lead to loss of tracking than in the case where the predicted curvature is nonzero. Thus an analysis of the straight line case will yield a bound on the parameters such that tracking will be guaranteed for *all* initial conditions.

Since x_d is a straight line with $\kappa_d = 0$ along the x -axis, its arclength parameter is simply $s_d = x$. From the straight line assumption, we trivially find that $x_d(s_d) = [s_d, 0]^T$. To simply notation we set $s_d = s$.

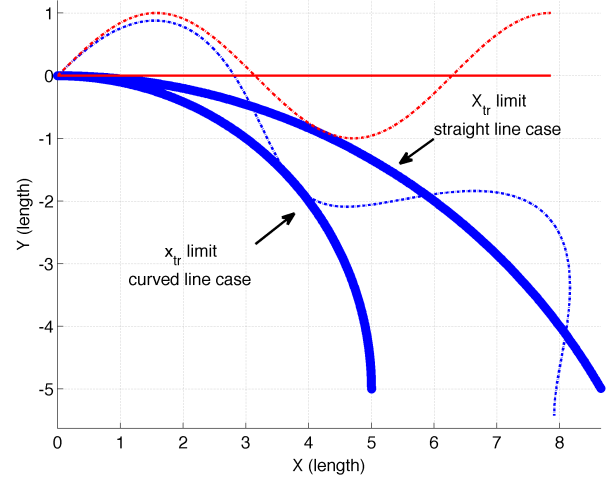


Fig. 6. Comparison of the limits of the κ_{tr} for a straight x_d case and a curved x_d case.

The AFM tip trajectory, generally obtained using (2), can be implemented by substituting $q_{2d} = [0, 1]^T$ to yield:

$$x_{tip}(s) = \begin{pmatrix} s \\ A \sin(\omega s) \end{pmatrix}. \quad (6)$$

To perform the “point match” condition, we need to find the equation for x_{tr} trajectory also. Assuming that we have the constant curvature κ_{tr} for the x_{tr} curve, the path is simply a circle with the radius of curvature of $R = 1/\kappa_{tr}$. Thus we describe the curve by the equation $x^2 + (y+R)^2 = R^2$. Substituting $x = s$ and re-arranging the standard circle equation to a vector form, we arrive at:

$$x_{tr}(s) = \begin{pmatrix} s \\ -R + \sqrt{R^2 - s^2} \end{pmatrix}. \quad (7)$$

We can now impose the full equation set of “point match” and “tangent match” as in (3), where we perform a standard derivative operation for the tangential vectors with respect to the only arclength parameter s . This yields:

$$\begin{pmatrix} s \\ A \sin(\omega s) \end{pmatrix} = \begin{pmatrix} s \\ -R + \sqrt{R^2 - s^2} \end{pmatrix} \quad (8a)$$

$$\arctan\left(\frac{1}{A\omega \cos(\omega s)}\right) = \arctan\left(\frac{1}{-s/\sqrt{R^2 - s^2}}\right) \quad (8b)$$

Using the same s to parameterize both the tip, (6), and true curves, (7), reduces the s_d and s_{tr} relationship to the trivial $s = s$.

Thus the four parameters A, ω, R and s are determined by (8). Note that we have two less unknown parameters less than the original full problem statement in

section (III-A). The assumption of a straight line forces κ_d to be zero and allows us to use only s to characterize both x_d and x_{tr} as oppose to having two independent parameters. There is an infinite number of solutions to these equations, corresponding the the equivalent set of conditions at each cycle of the sinusoid. We must then include the restriction that $\omega s \in [0, 2\pi]$.

We have also reduced the number of independent equations to two since the first component of (8a) is trivial. Thus we must still choose two of the parameters and solve for the remaining two. It is not physically meaningful to choose the value of s and thus the arclength value at the point of intersection is always a dependent variable. The choice of the other dependent variable depends upon the particular imaging problem. For example, given the samples to be imaged, physical models may constrain the maximum curvature, allowing us to choose R . Similarly there may be a predetermined imaging amplitude A determined by the maximum width of the string like-sample. The system (8) will then yield the necessary bound on the resolution parameter ω ; choosing a value equal to or larger than this bound will ensure tracking. Note that in this case the bound does not limit the resolution but instead limits the imaging time (since smaller values for ω imply that the sample will be traversed faster). In other situations it may be desirable to determine a bound on A in terms of given values of R and ω or on R in terms of A and ω .

IV. CONSERVATIVE BOUNDS

To yield insight into these bounds, as well as to derive a simple analytical result, we now consider a conservative bound by declaring tracking to be lost not at the point satisfying (3) but rather at the point given by $\omega s = 3\pi/2$. As illustrated in Fig. 7, this choice implies that the ‘‘tangent match’’ condition in (3b) is no longer satisfied.

With this assumption we are able to derive an analytical expression for the relationship between the parameters (see (10) below). To solve, first substitute $s_0 = \frac{3\pi}{2\omega}$ in the second equation of (8a), yielding

$$-A = -R + \sqrt{R^2 - \left(\frac{3\pi}{2\omega}\right)^2}.$$

Re-arranging, we find

$$A^2 - 2RA + \frac{9\pi^2}{4\omega^2} = 0. \quad (9)$$

We now have three unknowns, A , ω , and R and only one relationship, (9). To obtain the equations for one

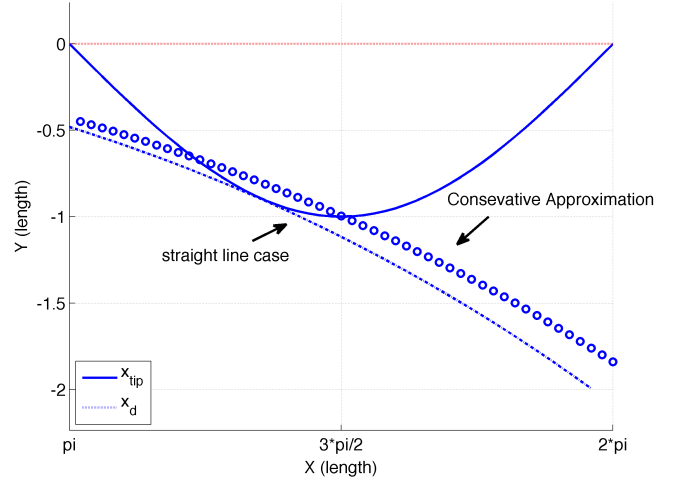


Fig. 7. Comparison of the conservative approximation of the two x_{tr} to the full solution in the straight line case. The conservative approximation declares tracking to be lost when the trajectory passes through the lowest point of the sine pattern. The true curve passing through this point has a smaller curvature than the curve that satisfies the point and tangent matching conditions. Thus solving for the parameters in the first case yield a conservative bound on the imaging parameters to guarantee tracking of the sample.

of the unknowns in terms of the other two, we simply re-arrange this equation, leading to:

$$A(R, \omega) = R - \sqrt{R^2 - \frac{9\pi^2}{4\omega^2}}, \quad (10a)$$

$$\omega(A, R) = \frac{1}{2} \sqrt{\frac{9\pi^2}{2RA - A^2}}, \quad (10b)$$

$$R(A, \omega) = \frac{A}{2} + \frac{9\pi^2}{8A\omega^2}. \quad (10c)$$

As before, two of the parameters can be chosen based on physical models of the system or other user insight. The equations in (10) then determine the bound on the third parameter to guarantee tracking of the sample. Due to the simplifications, these bounds are conservative. To consider the amount of conservatism introduced, we numerically solved the equations for the straight line case, (8) and compared the results to the analytical results of this section. In Fig. 8 we show the maximum curvature (one over the radius) of the true curve that will ensure tracking as a function of the resolution parameter ω for a fixed amplitude of one unit. For very small ω , only nearly straight lines can be tracked. As ω is increased, however, the limiting curvature increases to an asymptotic value. The conservative approximation, shown by the solid blue line, is clearly more cautious than the full solution. The

amount of conservatism introduced, however, is small.

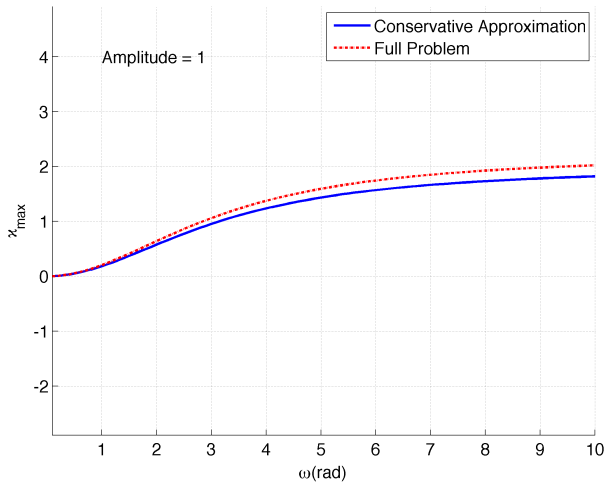


Fig. 8. Comparison of the conservative bound to the full solution for the straight line case. The scanning amplitude was fixed to one unit and the maximum curvature determined as a function of the resolution parameter ω . The level of conservatism introduced is small.

In Fig. 9 we fix the maximum curvature of the true curve at $\kappa = 1$ and explore the minimum value of the amplitude parameter A as a function of the resolution parameter ω . As before the level of conservatism introduced by the approximation is small.

V. CONCLUSION

In this paper we considered a non raster-scan algorithm for imaging string-like samples and described a scenario in which imaging could fail due to loss of tracking. We derived a set of equations that can be solved to yield bounds on the imaging parameters such that tracking is guaranteed. We then considered an extreme case to derive a somewhat simpler set of equations before deriving a set of conservative bounds on the parameters.

These results will be useful in applying the non-raster method to imaging samples and ensuring valid results in terms of the structure and length of the samples being studied.

ACKNOWLEDGEMENTS

This work was supported in part by a grant from the Agilent Foundation.

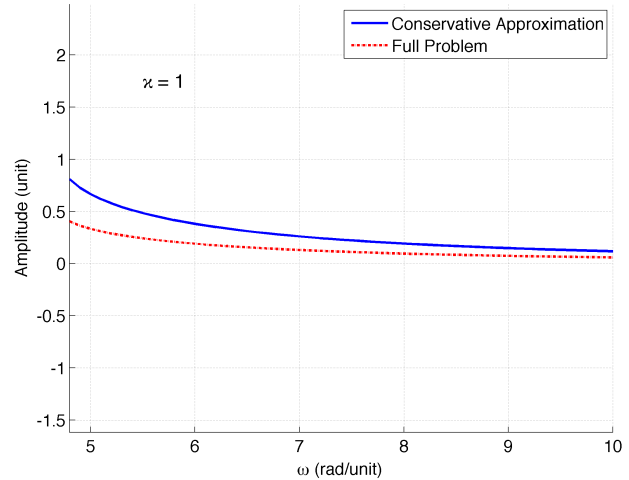


Fig. 9. Comparison of the conservative bound to the full solution for the straight line case. The curvature was fixed to one and the minimum amplitude determined as a function of the resolution parameter ω . As in Figure 8, the level of conservatism introduced by the simple bound is small.

REFERENCES

- [1] G. Binnig, C. F. Quate, and C. Gerber, "Atomic force microscope," *Phys. Rev. Lett.*, vol. 56, no. 9, pp. 930–933, March 1986.
- [2] N. C. Santos and M. A. R. B. Castanho, "An overview of the biophysical applications of atomic force microscopy," *Biophys. Chem.*, vol. 107, no. 2, pp. 133–149, February 2004.
- [3] A. Alessandrini and P. Facci, "AFM: a versatile tool in biophysics," *Meas. Sci. Tech.*, vol. 16, no. 6, pp. R65–R92, June 2005.
- [4] H. Janovjak, A. Kedrov, D. A. Cisneros, K. T. Sapra, J. Struckmeier, and D. J. Müller, "Imaging and detecting molecular interactions of single transmembrane proteins," *Neurobio. Aging*, vol. 27, no. 4, pp. 546–561, April 2006.
- [5] S. M. Salapaka and M. V. Salapaka, "Scanning probe microscopy," *Control Sys. Mag.*, vol. 28, no. 2, pp. 65–83, 2008.
- [6] K. K. Leang and A. J. Fleming, "High-speed serial-kinematic AFM scanner: design and drive considerations," in *Proc. American Control Conference*, 2008, pp. 3188–3193.
- [7] G. Schitter, K. J. Åström, B. E. DeMartini, P. J. Thurner, K. L. Turner, and P. K. Hansma, "Design and modeling of a high-speed afm scanner," *IEEE Trans. Control Sys. Techn.*, vol. 15, no. 5, pp. 906–915, September 2007.
- [8] T. Ando, T. Uchihashi, N. Kodera, D. Yamamoto, and A. Miyagi, "High-speed AFM and nanovisualization of biomolecular processes," *Euro. J. Physio.*, vol. 456, no. 1, pp. 211–225, 2008.
- [9] S. B. Andersson, "Curve tracking for rapid imaging in AFM," *IEEE Trans. Nanobio.*, vol. 6, no. 4, pp. 354–361, 2007.
- [10] P. I. Chang and S. B. Andersson, "Smooth trajectories for imaging string-like samples in afm: a preliminary study," in *Proc. American Control Conference*, Seattle, WA, June 2008, pp. 3207–3212.